Construction and analysis of ceRNA networks in the liver of black rockfish (Sebastes schlegelii) following Aeromonas salmonicida infection

Xiantong Liu
Qingdao Agricultural University
Ningning Wang
Qingdao Agricultural University
Haohui Yu
Qingdao Agricultural University
Xiaoyan Zhang
Qingdao Agricultural University
Chao Li
Qingdao Agricultural University
Min Cao (caomin@qau.edu.cn)
Qingdao Agricultural University

Research Article

Keywords: Sebastes schlegelii, Aeromonas salmonicida, liver, circRNA-miRNA-mRNA networks, immune response

Posted Date: July 24th, 2023

DOI: https://doi.org/10.21203/rs.3.rs-3166030/v1

Abstract

Given the dual roles in immune function and metabolism, liver can be selected as an interesting candidate to bridge host defense and metabolic adjustments during pathogen infections in teleost. In order to dissect the roles of liver in the immune response of *Sebastes schlegelii*, detection of activities of SOD, CAT and GPX4, systematic analysis of circRNA, miRNA and mRNA expression profiles, as well as circRNA-miRNA-mRNA regulatory networks in the liver of *S. schlegelii* following *Aeromonas salmonicida* infection were performed in the present study. The present results demonstrated the content of SOD, CAT and GPX4 increased significantly at early infection stage to protect the liver tissue from excessive damage. Meanwhile, 622 circRNA-miRNAs pairs, 78 miRNA-mRNA pairs and 327 circRNA-miRNA-mRNA pairs were identified in our study. These differently expressed circRNA and mRNA were related with LMNB1, DMBT1, NAMPT, IFIT1, CELSRs, PYGL etc. GO and KEGG enrichment analyses showed that differently expressed genes are related with TLR signal pathway, RIG signal pathway, PPAR signal pathway etc. These results revealed an antibacterial ceRNA network in the liver of *S. schlegelii* post *A. hydrophila* infection, which provided new clues and insights into the immune mechanisms of teleost.

1. Introduction

The liver is considered to be the main target organ that involved in metabolism. Because the liver is located in the abdominal cavity between the intestine and systemic circulation, it is constantly exposed to nutritional damage, intestinal microbiome products, and toxic substances (Freitas-Lopes MA et al., 2017). Once the nutrients are absorbed by the intestine and then were transported to the liver, which can then be responsible for filtering out excess harmful substances, thus acting as an immune modulator. Therefore, the liver not only performs metabolism-related functions, but also plays an important role in the body's immune function (Nemeth E et al., 2009). It has been demonstrated that the vertebrate liver can produce cytokines, chemokines, complement components and acute phase reactants proteins in response to pathogen infection (Robinson MW et al., 2016; Causey, Dwight R. et al., 2018). Given its dual roles in immune function and metabolism, liver can be selected as an interesting candidate to bridge host defense and metabolic adjustments during pathogen infections in teleost. For example, Castro et al. confirmed the presence of IgM^+, IgD^+, IgT^+, $CD8^{\alpha+}$, $CD3^+$ cells and cells expressing the major histocompatibility complex (MHC-II) in the liver of rainbow trout (*Oncorhynchus mykiss*), and evaluated the immune role of liver tissue in response to viral attack (Castro Rosario et al., 2014). Similarly, transcriptome analysis has been performed in *Epinephelus akaara*, immune-related genes such as *IL8, TLR9, CXCR4, CCL4*, and *IκBα* were found in the liver, suggesting the high carbohydrate level of diet can lead to inflammatory immune response in the liver of *E. akaara* (Yang Y et al., 2018). Therefore, identification of candidate genes involved in liver immunity and metabolism is the first step to elucidate its molecular mechanism.

High-throughput sequencing can provide detailed molecular information on global gene expression views, including the profiles of mRNA and non-coding RNAs (long ncRNAs (lncRNAs), circular RNAs (circRNAs) and microRNAs (miRNAs). Among these RNAs, the function of circRNA has been demonstrated that it

participates different biological processes via biding to miRNA as a sponge, thus to influence the expressions of the downstream target genes of miRNA and relevant signaling pathways (Cao M et al., 2021; Luo HL et al., 2021; Zheng W et al., 2022). In recent years, advances in high-throughput sequencing technology have resulted in the discovery of a large number potential regulatory pathways including lncRNA/circRNA-miRNA-mRNA in teleost. For instance, 1947 differentially expressed mRNAs, 9 differentially expressed miRNAs, and 4 differentially expressed circRNAs between fast- and slow-growing individuals of Nile tilapia were observed. Based on the constructed ceRNAs, circMef2c can interact with 3 miRNAs and 65 mRNAs that regulate growth, thus providing novel insights into the role of circRNAs in the regulation of muscle growth in teleost (Golam Rbbani et al., 2023). In teleost fish, infection-associated ceRNAs have been reported in a number of species. Cai et al. investigated the whole-transcriptome in the in the *Vibrio anguillarum* infected turbot liver, and constructed miRNA-circRNA pairs, miRNA-mRNA pairs and 65 circRNA-miRNA-mRNA pairs. They speculated that novel_circ_0002878/miR-34a/NR1D2 axis may relate with protection against bacterial infection (Cai X et al., 2022). Researchers studied the expression profiles of circRNAs, miRNA and mRNA in *S. schlegelii* response to *Edwardsiella tarda* infection, and identified ceRNAs networks that are strongly related to immune signaling pathways, such as the NF-κB signal pathway and the chemokine signaling pathway (Cao M et al., 2021). In addition, the whole-transcriptome sequencing was conducted in the black rockfish spleen with *Aeromonas salmonicida* challenging to construct circRNA-miRNA-mRNA networks. Totally, 290 circRNA-miRNA-mRNA pathways were constructed including 31 circRNAs, 50 miRNAs, and 156 mRNAs, which can regulate immune related genes and signal pathways such as immunoglobulin, mucin domain-containing protein 4, Galectin-9 and Cathepsin D, FoxO signaling pathway, Jak-STST signaling pathway, TGF-β signaling pathway, etc. (Gao C et al., 2023). However, studies on the interactions of mRNAs and ncRNAs in the liver of *S. schlegelii* response to *A. salmonicida* have not been carried out systematically.

The black rockfish (*S. schlegelii*), which inhabits the coastal waters of China, Japan, and Korea, has been studied extensively due to its viviparous breeding habits and aquaculture requirements. However, the aquaculture of *S. schlegelii* still has many shortcomings such as low level of farming intensification, inadequate breeding techniques and degradation of germplasm resources, which have directly led to decrease in its growth rate, disease resistance and mortality. Liver plays an important role in fish metabolism, immune defense and life activities. Therefore, *S. schlegelii* was selected as the object to explore the changes in the activities of Glutathione peroxidase 4 (GPX4), superoxide dismutase (SOD) and catalase (CTA) in liver and the whole transcriptome expression characteristics following *Aeromonas salmonicida* infection at different time points. The purpose of this study is to investigate the immune response of *S. schlegelii* to bacterial infection based on the gene expressions as well as activities of enzyme.

2. Materials and methods

2.1 Ethics approval and consent to participate

The protocol was approved by the Committee on the Ethics of Animal Experiments of Qingdao Agricultural University IACUC (Institutional Animal Care and Use Committee).

2.2 Sample collection and bacterial infection

The experimental healthy fish were obtained from a local fish farm in Weihai, Shandong Province. Firstly, fish were acclimated in a recirculating fresh water system for one week before bacterial infection experiments was conducted. For bacterial infection, fish in the experimental groups were challenged in 30 L (20 L water) aquaria in triplicates, and each replicate was consisted of 5 random individuals. Individuals were immersed in *A. salmonicida* for 2 h at a final concentration of 5-6 × 10^7 CFU/mL. Then, the liver tissues from 5 fish were collected as one sample at 2 h (AS2H), 12 h (AS12H) and 24 h(AS24H) after euthanized with MS-222 (200 mg/L). Meanwhile, fish in seawater were defined as the control (CON) group. All samples were flash frozen in liquid nitrogen and stored at − 80 °C for RNA extraction.

2.3 Measuring of the activities of SOD, CAT and GPX4 enzyme

After tissue collection from different time points, 0.1 of liver sample of the *A. salmonicida* infected *S. schlegelii* was ground in 2 mL of 50 mM (containing 0.2 mM EDTA) phosphate-buffered saline (PBS; pH 7.8). The homogenate was then transferred to a test tube and centrifuged at 12,000 rpm for 20 min. After centrifugation, the supernatant was collected as the enzymatic solution for the following measurement of the activities of SOD, CAT and GPX4 enzyme. The activities of SOD, CAT and GPX4 enzyme were detected by using a SOD kit (Jiancheng, A007-2-1), CAT (Jiancheng, A001-1) and GPX4 kit (Jiancheng, H545-1-1), respectively.

2.4 Library construction and sequencing

Total RNA was extracted from CON and infected liver samples with TRIzol Reagent (Invitrogen, Carlsbad, CA, USA) according to the instructions. The purity, and integrity of extracted RNA were detected using NanoPhotometer spectrophotometer (IMPLEN, CA, USA) and Agilent 2200 TapeStation (Agilent Technologies, USA), respectively. Subsequently, the library construction, sequencing, gene expression levels quantification, ceRNA networks constructions, and functional analysis have been described in a previous study (Cao M et al., 2021).

2.5 qRT-PCR verification of the expressions of circRNA, miRNA and mRNA in the networks

To validate the accuracy of RNA sequencing, we detected the expression levels of 30 DE-RNAs, including 10 DE-circRNAs, 10 DE-miRNAs, and 10 DE-mRNAs by qRT-PCR, as well as compared the expression patterns with those from RNA sequencing results. RNA samples were used from the same sample that used for sequencing library construction. For all the primers of DE-mRNAs and DEcircRNAs used in this study, PrimerQuest (https://sg.idtdna.com/PrimerQuest/Home) was used for these primers design. For miRNA primers, they were designed on the basis of the instructions of miRcute miRNA isolation kit (Tiangen Biotech, China). Subsequently, β-actin was chosen as an internal control to normalize the

relative quantification of circRNAs, and mRNAs, while U6 was used as an internal control of miRNA. The used primers in this study were listed in Table 1. Then, expression profiles of the selected-genes were analyzed with a CFX96 real-time PCR detection system (Bio-Rad Laboratories, Hercules, CA, USA) as descripted in previous study (Cao et al., 2020). Finally, the $2^{-\Delta\Delta Ct}$ method (Livak KJ et al.,2001) was used to calculate the relative expression levels and the data were expressed as the mean SE of three replicates.

Table 1 Primers used in the current study

Primer	Sequence (5’-3’)
dre-miR-155	TTAATGCTAATCGTGATAGGGG
dre-miR-190a	TGATATGTTTGATATATTAGGT
dre-miR-22a-3p	AAGCTGCCAGCTGAAGAACTGT
dre-let-7b	TGAGGTAGTAGGTTGTGTGGTT
dre-miR-301b-5p	GCTTTGACGATGTTGCACTAC
dre-miR-128-3p	TCACAGTGAACCGGTCTCTTTT
novel_169	TCAGGAGTTTTAGAAATCGGTG
novel_559	TAGGACAATAATTAAGGCAGA
dre-miR-456	CAGGCTGGTTAGATGGTTGTCA
dre-miR-20a-5p	TAAAGTGCTTATAGTGCAGGTAG
TCONS_00098868F	TGTACGATGGATGCCGTAAAG
TCONS_00098868R	GGATCAGCTTTGAACAGGAAATG
TCONS_00019905F	CAAACATGGTGGCCCTTTAATC
TCONS_00019905R	CAGCCATCTTCAGGGTCATATC
TCONS_00070177F	AGTCTGGTGGTTCTGCTTTC
TCONS_00070177R	TCTGCTGTGACCTTCTGTAATG
TCONS_00113123F	CCCGTGTCTTTCTACCTCTTTC
TCONS_00113123R	CGACTTCGGCAGAGTCAAAT
TCONS_00088456F	CTGAGGAGGAGATGTGAATGTG
TCONS_00088456R	ACTCTGTCCCTCTGTGATGTA
TCONS_00009109F	GACTGCTACAACCACGACTAC
TCONS_00009109R	GCTCTCAGTCCACAACCATT
TCONS_00044066F	GTGAGGGCTGTTTGTTAGGA
TCONS_00044066R	CGCCCTCACCACCATTATTA
TCONS_00002961F	GTCGTGGTTACCAGGTGTATAAG
TCONS_00002961R	CGATGGTCTTAACCTCGTTCTC
evm.model.Chr11.381F	ACAATGTCGGGTTCCTCTAATC
evm.model.Chr11.381R	GGGAGACCTTCACTCTGTTTATG
TCONS_00090561F	GTTGCTCAGCTGGTCTGATAG

TCONS_00090561R	TGACTGACTGCTGGATGATTG
novel_circ_0000790F	ACCTCTCGGCTGTCTGTAT
novel_circ_0000790R	CAGCTCATTGAAGCGGATTTG
novel_circ_0000829F	TTACCTCTACCCAGATCCATCC
novel_circ_0000829R	AGTGCAGTTAGACACCCAATAC
novel_circ_0000791F	GCACAGAGAAGAAGAGTGTGAG
novel_circ_0000791R	GAAGAGGGAGGAGGAGAGAAG
novel_circ_0000320F	TTGGGTCTGAAGGTCAAAGAG
novel_circ_0000320R	GGTGGAGTAGGACAGGTAGAA
novel_circ_0000773F	TGTGGGATTCCTCCTCTCAA
novel_circ_0000773R	GGGACACTCTCTCTCCAATCT
novel_circ_0001459F	CACCAACAACACCGAATGTG
novel_circ_0001459R	CTCCCTGTGTGGCATCTTATC
novel_circ_0000343F	TTGGAGGACGTGAAGAGTTTG
novel_circ_0000343R	ACAAGTGATGTAGGACGGATTG
novel_circ_0001460F	CCAGTCTGTGCTTTCCAGAT
novel_circ_0001460R	AGCAGTTGTGTTTGTGTTTCC
novel_circ_0000004F	GGATGGAGAGCACGACAAA
novel_circ_0000004R	CAGTTCTTCCTCCGGATCTTATC
novel_circ_0000298F	GGAACACGCCGATAGAAGAG
novel_circ_0000298R	CCAGCAGGTGGGATGTATTT

2.6. Data analysis

The physiological and biochemical indexes and fluorescence quantitative experiments were repeated for 3 times. SPSS 20.0 was used for statistical significance analysis, and the data were expressed as mean ± standard deviation. $p < 0.01$ is considered to be a significant difference and $p < 0.05$ was considered a significant difference.

3. Results

3.1 Activities of SOD, CAT and GPX4 enzyme

The activities of SOD, CAT and GPX4 enzyme in control and *A. salmonicida* infected livers of *S. schlegelii* was shown in Figure 1. The activity of CAT in the liver of healthy fish (0 h) was 83.32±2.65 U/gHb. When infected with *A. salmonicida,* the content of CAT in *S. schlegelii* liver was reached the highest level of 127.20±8.25 U/gHb after 2 h infection, and then decreased in the other infected groups. In detail, the activities of CAT were 115.21±1.88 U/gHb at 12 h and reached the lowest level (80.95±7.70 U/gHb) at 24h after infection (Figure 1 A). We also noticed that the activity of GPX4 was 5.32±0.59 mg/ml at 0 h, increased to 5.75±0.30 mg/ml at 2 h after infection, and then continued to increase, reaching the highest level at 12 h (5.83±0.23 mg/ml) (Figure 1 B). Similarly, the activity of GPX4 also decreased at 24 h (4.86±0.36 mg/ml). SOD activity was 6.26±0.58 U/ml at 0 h, reached the highest level (6.87±0.82 U/ml) at 2 h after infection. While, the SOD decreased less than that in the control (0 h) at 12 h and 24 h (Figure 1 C).

3.2 Transcriptome sequencing results of circRNAs

In order to fully understand the circRNAs in response to *A. salmonicida* infection of *S. schlegelii*, the rRNA-depleted samples from control and *A. salmonicida* infected liver samples at different infection time points (2, 12 and 24 h) were used to library construction and sequencing. A total of 2,406 circRNAs were identified in *S. schlegelii* and widely distributed on different chromosomes (Figure 2A). 71.60%, 0.22% and 0.07% identified circRNAs were generated from exons, intergenic and intron, respectively (Figure 2B). The length distribution of circRNAs were mainly ranged from 200 to 400 bp (Figure 2C). As shown in Figure 2D, the expression patterns of the *A. salmonicida*-infected and control samples were categorized into different clusters. The results of circRNAs expression patterns showed that a total of 3, 6 and 11 DE-circRNAs were identified in *A. salmonicida*-infected groups (AS2H, AS12H, and AS24H) against the control group (Figure 2E). Functional analysis was performed to clarify the biological function of circRNAs of *S. schlegelii* after *A. salmonicida* infection (Figure 2F, 2G). The results showed that the DE-circRNAs were involved in multiple biological processes such as protein processing in edoplasmic reticlum, mTOR signaling pathway, MAPK signaling pathway, insulin signaling pathway, herpes simplex infection, FoxO signaling pathway, adherens junction.

3.3. Transcriptome sequencing results of miRNAs

For small RNA, the length of these miRNAs was mainly ranged from 21 to 23 nt, and the length of 22 nt showed the peak distribution (Figure 3A). A total of 473 miRNAs were obtained, including 231 known miRNAs and novel 242 miRNAs (Figure 3C). Among which16 (AS2H), 22 (AS2H) and 57(AS2H) differentially expressed miRNAs, respectively (Figure 3B). The top DE-miRNAs were presented in a heat map based on gene expression (Figure 3D). In order to explore the functions of these DE-miRNAs furtherly, GO and KEGG were used to perform statistical analysis of their target genes. The target genes were mainly enriched in 2,436 GO term processes (Figure 3E). KEGG analysis showed that the target genes of DE-miRNAs were involved in wnt signaling pathway, focal adhesion and adrenergic signaling in caridiomyocytes (Figure 3F).

3.4 Statistical Analysis of mRNAs Data

A total of 6,745 significantly DEmRNAs were identified by stringent thresholds (FDR< 0.05), among which 3,694 DEmRNAs were upregulated, and 3,052 DEmRNAs were downregulated (Figure 4A). We also found that 14 core genes were expressed differently at each time point of infection, and 27, 2,460 and 1,618 genes that specific to AS2H, AS12H and AS24H, respectively (Figure 4B). Then, the function of DE-mRNA was analyzed by GO analysis and KEGG pathway analysis showed that most DE-mRNAs participate metabolic process. In addition, we also noticed some genes are related with TLR signal pathway, RIG signal pathway, PPAR signal pathway etc (Figure 4C-D).

3.5 Construction of the circRNA-miRNA, miRNA-mRNA, and ceRNA regulatory networks

Among ncRNAs, circRNAs can regulate the gene expression on post-transcriptional levels by sponging miRNAs. Meanwhile, miRNAs can bind to the 3' UTR of mRNAs or the coding regions to repress or degrade the mRNAs, thus influencing the expression of relative genes. Therefore, the circRNA-miRNA, miRNA-mRNA, and ceRNA regulatory networks during the infection of *A. salmonicida* in the liver of *S. schlegelii* were analyzed. Totally, 622 circRNA-miRNAs pairs were identifed in our study, including 164 circRNAs and 175miRNAs (Table S1). And, 78 miRNA-mRNA pairs were identified, including 43 miRNA and 69 mRNA (Table S2). The ceRNA regulatory network contained 327 circRNA-miRNA-mRNA pairs, including 31 circRNAs, 35 miRNAs, and 31 mRNAs (Figure 5 and Supplementary Table S3). Among which, we found that novel_circ_0000320/dre-let-7b/evm.model.Chr1.63 (Lamin-B1, LMNB1), novel_circ_0000320/dre-let-7a/TCONS_00113123(GTPase IMAP family member 8-like, GIMAP8), novel_circ_0001251/dre-miR-187/evm.model.Chr1.2451(FERM domain-containing protein 4B, FRM4B), novel_circ_0000773/dre-miR-100-5p/TCONS_00017916(collagenase 3-like), dre-miR-145-3p/novel_circ_0000748/TCONS_00097654(deleted in malignant brain tumors 1 protein-like, DMBT1)), novel_circ_0001351/dre-miR-18a/TCONS_00116969(dixin-A-like), novel_circ_0000791/dre-miR-22a-3p/evm.model.Chr1.1161(Nicotinamide phosphoribosyltransferase, NAMPT), novel_circ_0001377/novel_215/evm.model.Chr1.1906(Cadherin EGF LAG seven-pass G-type receptor 2, CELR2), novel_circ_0000790/dre-miR-155/TCONS_00116969 (3-oxoacyl-[acyl-carrier-protein] reductase, FabG-like), novel_circ_0001459/dre-miR-128-3p/TCONS_00078350(ubiquitin carboxyl-terminal hydrolase 47-like, USP47), novel_circ_0001387dre-miR-140-5p/TCONS_00102560 (interferon-induced protein with tetratricopeptide repeats 1-like, IFIT1), novel_circ_0000004/dre-miR-456/evm.model.Chr11.381(Guanine nucleotide-binding protein,GBG5), novel_circ_0001880/novel_182/evm.model.Chr15.1085(Glycogen phosphorylase, PYGL), novel_circ_0000791/dre-miR-22a-3p/evm.model.Chr16.719 (Pumilio homolog 1, PUM1), novel_circ_0000342/dre-miR-22b-3p/evm.model.Chr3.156 (Myotubularin-related protein 7, MTMR7), novel_circ_0001377/novel_215/evm.model.Chr24.291(Neural-cadherin, CADN) etc. These circRNA-miRNA-mRNA networks can be chosen as candidates for functional analysis in the future.

3.6 Validation of circRNAs, miRNAs and mRNAs by qRT-PCR

In order to verify the authenticity of the DE-circRNAs, DE-miRNAs and DE-mRNAs that identified from the transcriptome data of *S. schlegelii* after *A. salmonicida*, 10 differentially expressed circRNAs were selected. The qPCR results confirmed that the expression patterns of the selected circRNAs were

consistent with the sequencing results. We noticed that most of the 10 detected circRNAs were up-regulated in *S. schlegelii* after *A. salmonicida*. For example, the expression of novel_circ_0000298F increased by 3.23 fold, 3.24 fold and 3.79 fold at 2 h, 12 h and 24 h after infection, respectively. novel_circ_0000343F expression was up-regulated 4.78 fold at 2 h after infection, 3.51 fold at 12h after infection, and 2.26 fold at 24h after infection. While, the expression of novel_circ_0000773F was decreased by 0.55 fold at the initial stage of infection, and showed an upward trend with the increase of infection time (Figure 6). Meanwhile, the similar expression trends between sequencing analysis and qRT-PCR of 10 miRNAs were present though there were few differences in the fold change of expressions. miRNAs changed significantly after infection. For example, the expression of re-let-7b showed an up-regulation trend at all time points, and the up-regulation rate was 46.49 fold at 2 h after infection, 282.76 fold at 12 h after infection, and 265.06 fold at 24 h after infection. The expression of dre-miR-190a was down-regulated by 0.34 fold at 2 h after infection, up-regulated by 4.94 fold at 12h after infection, and down-regulated by 0.59 fold at 24 h after infection (Figure 7). The qRT-PCR results confirmed that the expression patterns of the mRNAs were consistent with the sequencing results (Figure 8). Different mRNAs showed different expression patterns during infection. For example, the expression level of TCONS_00002961 showed an up-regulated trend at all time points after infection, and was up-regulated 1.07 fold, 1.18 fold, and 2.22 fold at 2 h, 12 h, and 24 h after infection, respectively. However, the expression of TCONS_00019905 was up-regulated by 1.36fold at 2 h after infection, and down-regulated at 12 h and 24 h by 0.51 fold and 0.32 fold, respectively.

Discussion

S. schlegelii is a demersal fish widely distributed in the northwest Pacific along the coast of China, Japan and the Korean Peninsula (Wang L et al., 2017). The current research on *S. schlegelii* mainly focuses on its growth, behavior, physiology, immunity and population genetics (Gao Y et al., 2023; Gao Y et al., 2023; Yin L et al.,2018; Cao M et al., 2023). It has been reported that bacterial and viral pathogens threatened the yield of *S. schlegelii*. Among many pathogenic bacteria, *A. salmonicida* is the causative agent to be linked to fish disease that characterized by high mortality and morbidity (Menanteau-Ledouble S et al., 2016). It has been mentioned that the liver is the primary immune tissue of teleost in defensing against pathogentic infections (Nemeth E et al., 2009). In order to understand the immune response mechanisms of liver in this species, the activities of GPX4, SOD and CTA in the liver, as well as whole transcriptome analysis in *S. schlegelii* after challenge with *A. salmonicida* were investigated. These results can provide novel knowledge about ncRNAs in immune responses process in *S. schlegelii*, and will serve as important resources for further investigating the roles of ncRNAs during pathogen infections in teleost.

In this study we investigated the effects of *A. salmonicida* on the livers of *S. schlegelii*, and detected the activities of SOD, CAT and GPX4. The present results demonstrated the content of SOD, CAT and GPX4 increased significantly at early infection stage. It has been reported the antioxidant enzyme defense system involves SOD, CAT, GPX and glutathione reductase (GSR) (Papas M et al., 2019). CAT is the hallmark enzyme of peroxisome that widely existed in prokaryotes and eukaryotes, accounting for about

40% of the total peroxisome enzymes, and is one of the key enzymes in the biodefense system established during the process of biological evolution. The enzyme can work with GPX to remove hydrogen peroxide produced by superoxide dismutase dismutating superoxide anion from the free groupand protect cells from the poison of peroxide (Cerutti P et al.,1994). We thus hypothesized that in the initial stages of infection, the activity of these three enzymes increases rapidly, interacting with reactive oxygen species in *S. schlegelii* to protect the liver tissue from excessive damage.

There is increasing evidence demonstrated that activation and termination of immune response are regulated at multiple levels, including transcriptional and post-transcriptional levels. At transcriptome level, total 6748 mRNAs were induced differential expression following *A. salmonicida* challenge. A mass of them were regarded as immune-related genes, such as apoptosis, C-X-C motif chemokines, cell adhesion molecules, RIG-I-like receptor, TLR-like receptor, NOD-like receptor etc. The results demonstrated that these DE mRNAs were induced to participate in a series of biological processes and played immune roles against the invasion of *A. salmonicida*. At post-transcriptional level, ncRNAs (circRNA, miRNA and lncRNA) were involved in the interactions between pathogens and teleost (Wang M et al., 2018). Among which, circRNAs or lncRNAs can competitively bind miRNAs to achieve the purpose of regulating mRNA levels (Robles V et al., 2019). Totally, 622 circRNA-miRNAs pairs, 78 miRNA-mRNA pairs were identified in our study. Among which, several key immune response pathways regulated by circRNAs and miRNAs were found through functional enrichment analysis. For example, the JAK/STAT signaling pathway, p53 signaling pathway, Wnt signaling pathway and Toll-like receptor signaling pathway play crucial roles in the immune system (Xin P et al., 2020; Rivas C et al., 2010; El-Sahli S et al., 2019; Kawasaki T et al., 2014). Moreover, target genes of DE miRNAs that related with fatty acid degradation, as well as other glycan degradation also been found in the liver of *S. schlegelii*. It has been reported that the degradation of fatty acids is mainly in the liver, mainly because the liver plays a vital role in lipid metabolism (Volpe J J et al., 1973). Additionally, we identified several miRNAs that related to SOD, CAT and GPX4 according to the function of target genes. For example, the downregulation of novel_11, dre-miR-205-5p and dre-miR-301b-5p may related to the upregulation of SOD, CAT and GPX4, respectively. We thus speculated that these miRNAs can regulate the expression and content of SOD, CAT and GPX4.

Previous study showed that the liver harbors populations of immune cells that contributing to liver immune function including monocytes, macrophages, neutrophils, B lymphocytes, T lymphocytes, NK cells and NKT cells in the body (Freitas-Lopes MA et al., 2017). Based on the transcriptome sequencing technology, numbers of non-coding RNA and mRNA networks were identified in the liver of teleost. For example, in the infected liver of *blunt snout bream,* the parental genes of 106 differentially expressed circRNAs were enriched in phagocytosis, complement and coagulation cascades, and Fc gamma R-mediated phagocytosis pathways (Wang G et al., 2021). Cai et al. performed a comprehensive analysis of whole-transcriptome sequencing in the turbot liver following *V. anguillarum* infection, and identified 65 circRNA-miRNA-mRNA networks that related with TRI25, NR1D2; CMTA1; and MGLL (Cai X et al., 2023). In our study, we totally identified 327 circRNA-miRNA-mRNA regulatory networks including 31 circRNAs, 35 miRNAs, and 31 mRNAs. Among which, LMNB1 was predicted to be regulated by novel_circ_0000320 and dre-let-7b. It has been reported that LMNB1 is a major structural component of the nucleus that appears

to be involved in the regulation of many nuclear functions (Shimi T et al., 2011). The “up-down-up” relationships of novel_circ_0000320/dre-let-7b/ LMNB1 suggested that the novel_circ_0000320 can release the inhibition of dre-let-7b and promote the expression of LMNB1.We also found that the expression of DMBT1 was regulated by dre-miR-145-3p, whereas dre-miR-145-3p can be sponged by circRNA novel_circ_0000748. DMBT1 is a natural defense protein involved in innate immunity, inflammation and epithelial cell differentiation, and plays an important role in diseases associated with pathological processes (Müller H et al, 2015). We found that NAMPT can be induced and regulated by novel_circ_0000791 and dre-miR-22a-3p in the infected liver. NAMPT, also known as pre-B cell clonal enhancer factor and visceral adipose hormone, has become a research hotspot in the fields of nicotinamide adenine dinucleotide biology, metabolism and inflammation due to its various functions in recent years (Imai S, 2009). Moreover, we found that dre-miR-140-5p acts as an inhibitor of IFIT1, which is regulated by interferon, a variety of viruses and some pathogen-related molecular patterns, which can inhibit viral replication and inhibit inflammatory response (Zhou X et al., 2013). Our results showed that under the regulation of circRNAs and miRNAs, CELSRs participated the cell differentiation and cell contaction in the liver, which involved in many biological processes during embryonic development, such as neuronal/endocrine cell differentiation, vascular valve formation, cell adhesion, and control of planar cell polarity (Wang XJ et al.,2014). Additionally, the “down-up-down” expression patterns of novel_circ_0001880/novel_182/PYGL indicated that gene related to glycogen metabolism was inhibited, and circRNAs and miRNAs participate in this regulatory process. GO and KEGG enrichment analyses showed that differently expressed genes are related with TLR signal pathway, RIG signal pathway, PPAR signal pathway etc. These results revealed an antibacterial ceRNA network in the liver of *S. schlegelii* post *A. hydrophila* infection, which provided new clues and insights into the immune mechanisms of teleost.

Conclusion

In conclusion, we investigated the circRNA, miRNA and mRNA expression profiles of the *S. schlegelii* liver that challenged with *A. hydrophila* in this study, which expanded our understanding of ceRNAs and their roles in teleost. We further predicted immune genes are regulated at the transcriptional level and post-transcriptional level in the process of liver infection by pathogenic bacteria based on the constructed networks. Meanwhile, activities of antioxidant enzymes, fatty acid metabolism and glycogen metabolism in the liver are also affected. These results provide new information for the study of the regulatory mechanisms of immune response of liver in teleost after bacterial infection.

Declarations

Author contributions

Xiantong Liu and Ningning Wang analyzed the results and wrote this paper; Xiantong Liu and Haohu Yu collected materials and performed the bacteria challenge experiment; Xiaoyan Zhang analyzed the sequencing results of circRNA, miRNA and mRNA; Min Cao performed the histopathological analysis on

the intestine tissues and revised the manuscript; Chao Li conceived, designed the research and revised the manuscript.

Funding

This work was supported by the Young Experts of Taishan Scholars (NO.tsqn201909130), and Shandong Technical System of Fish Industry (SDAIT-12-03).

Competing interests: The authors declare that there is no conflict of interest.

Availability of data: Not applicable.

References

1. Cai X, Gao C, Lymbery AJ, Armstrong NJ, Ma L, Li C. The immune-related circRNA-miRNA-mRNA ceRNA regulatory network in the liver of turbot (*Scophthalmus maximus L.*) induced by *Vibrio anguillarum*[J]. Fish Shellfish Immunol,2023, 132:108506.
2. Cao M, Xue T, Huo H, Zhang X, Wang NN, Yan X, Li C. Spatial transcriptomes and microbiota reveal immune mechanism that respond to pathogen infection in the posterior intestine of *Sebastes schlegelii*[J]. Open Biol,2023,13(2):220302.
3. Cao M, Yan X, Su B, et al. Integrated analysis of circRNA-miRNA-mRNA regulatory networks in the intestine of *Sebastes schlegelii* following *Edwardsiella tarda* challenge[J]. Front Immunol ,2021,11:618687.
4. Causey DR, Kim JH, Stead DA, Martin SAM, Devlin RH, Macqueen DJ. Proteomic comparison of selective breeding and growth hormone transgenesis in fish: Unique pathways to enhanced growth[J]. J Proteomics,2019,192:114–124.
5. Cerutti P, Ghosh R, Oya Y, Amstad P. The role of the cellular antioxidant defense in oxidant carcinogenesis[J]. Environ Health Perspect,1994,102 Suppl 10(Suppl 10):123–129.
6. Freitas-Lopes MA, Mafra K, David BA, Carvalho-Gontijo R, Menezes GB. Differential Location and Distribution of Hepatic Immune Cells[J]. Cells. 2017,6(4):48.
7. Gao C, Cai X, Ma L, Sun P, Li C. Systematic analysis of circRNA-related ceRNA networks of black rockfish (*Sebastes schlegelii*) in response to *Aeromonas salmonicides* infection[J]. Fish Shellfish Immunol, 2023,135:108648.
8. Gao Y, Han G, Qiang L, et al. Hematological varieties, histological changes, and immune responses in the early stage of infection with *Vibrio parahaemolyticus* in black rockfish *Sebastes schlegelii*[J]. Aquaculture International, 2023, 31(1): 381–399.
9. Gao Y, Li Z, Han G, Qiang L, Sun Y, Tan R, Yu Y. Effects of the water-soluble fraction of diesel oil on the sera biochemical indicators, histological changes, and immune responses of black rockfish *Sebastes schlegelii*[J]. Mar Environ Res,2023 ,187:105953.

10. Livak KJ, Schmittgen TD. Analysis of relative gene expression data using real-time quantitative PCR and the 2(-Delta Delta C(T)) Method[J]. Methods ,2001,25(4):402–408.
11. Imai S. Nicotinamide phosphoribosyltransferase (Nampt): a link between NAD biology, metabolism, and diseases[J]. Curr Pharm Des,2009;15(1):20–28.
12. Luo HL, Pi J, Zhang JA, Yang EZ, Xu H, Luo H, Shen L, Peng Y, Liu GB, Song CM, Li KY, Wu XJ, Zheng BY, Shen HB, Chen ZW, Xu JF. Circular RNA TRAPPC6B inhibits intracellular *Mycobacterium tuberculosis* growth while inducing autophagy in macrophages by targeting microRNA-874-3p[J]. Clin Transl Immunology,2021,10(2):e1254.
13. Robinson MW, Harmon C, O'Farrelly C. Liver immunology and its role in inflammation and homeostasis[J]. Cell Mol Immunol,2016,13(3):267–276.
14. Menanteau-Ledouble S, Kumar G, Saleh M, El-Matbouli M. *Aeromonas salmonicida*: updates on an old acquaintance[J]. Dis Aquat Organ,2016,120(1):49–68.
15. Müller H, Nagel C, Weiss C, Mollenhauer J, Poeschl J. Deleted in malignant brain tumors 1 (DMBT1) elicits increased VEGF and decreased IL-6 production in type II lung epithelial cells[J]. BMC Pulm Med,2015,15:32.
16. Nemeth E, Baird AW, O'Farrelly C. Microanatomy of the liver immune system[J]. Semin Immunopathol,2009 ,31(3):333–343.
17. Papas M, Arroyo L, Bassols A, Catalán J, Bonilla-Correal S, Gacem S, Yeste M, Miró J. Activities of antioxidant seminal plasma enzymes (SOD, CAT, GPX and GSR) are higher in jackasses than in stallions and are correlated with sperm motility in jackasses[J]. Theriogenology, 2019,140:180–187.
18. Rbbani G, Nedoluzhko A, Siriyappagouder P, Sharko F, Galindo-Villegas J, Raeymaekers JAM, Joshi R, Fernandes JMO. The novel circular RNA CircMef2c is positively associated with muscle growth in *Nile tilapia*[J]. Genomics, 2023 ,115(3):110598.
19. Rivas C, Aaronson SA, Munoz-Fontela C. Dual role of p53 in innate antiviral immunity[J]. Viruses,2010 ,2(1):298–313.
20. Robles, V., Valcarce, D. G., & Riesco, M. F. Non-coding RNA regulation in reproduction: Their potential use as biomarkers[J]. Non-Coding RNA Research, 2019,4(2), 54–62.
21. Castro, R., Abós, B., Pignatelli, J., von Gersdorff Jørgensen, L., González Granja, A., Buchmann, K., & Tafalla, C. Early immune responses in rainbow trout liver upon *Viral Hemorrhagic Septicemia Virus* (VHSV) Infection[J].Plos One, 2014, 9(10):e111084.
22. Shimi T, Butin-Israeli V, Adam SA, Hamanaka RB, Goldman AE, Lucas CA, Shumaker DK, Kosak ST, Chandel NS, Goldman RD. The role of nuclear lamin B1 in cell proliferation and senescence[J]. Genes Dev,2011,25(24):2579–2593.
23. Volpe J J, Lyles T O, Roncari D A K, et al. Fatty acid synthetase of developing brain and liver: content, synthesis, and degradation during development[J]. Journal of Biological Chemistry, 1973, 248(7): 2502–2513.
24. Wang G, Sun Q, Wang H, Liu H. Identification and characterization of circRNAs in the liver of blunt snout bream (*Megalobrama amblycephala*) infected with Aeromonas hydrophila[J]. Dev Comp

Immunol,2021,124:104185.

25. Wang, L., Wu, Z., Liu, M. et al. Length-weight, length-length relationships, and condition factors of black rockfish *Sebastes schlegelii* Hilgendorf, 1880 in Lidao Bay, China[J]. Thalassas ,2017,33: 57–63.
26. Wang M, Jiang S, Wu W, Yu F, Chang W, Li P, Wang K. Non-coding RNAs Function as Immune Regulators in Teleost Fish[J]. Front Immunol,2018,9:2801.
27. Wang XJ, Zhang DL, Xu ZG, Ma ML, Wang WB, Li LL, Han XL, Huo Y, Yu X, Sun JP. Understanding cadherin EGF LAG seven-pass G-type receptors[J]. J Neurochem,2014,131(6):699–711.
28. Xin P, Xu X, Deng C, et al. The role of JAK/STAT signaling pathway and its inhibitors in diseases[J]. International Immunopharmacology,2020,80:106210.
29. Yang Y, Han T, Xiao J, Li X, Wang J. Transcriptome analysis reveals carbohydrate-mediated liver immune responses in *Epinephelus akaara*[J]. Sci Rep. 2018,8(1):639.
30. Yin L, Chen B, Xia B, Shi X, Qu K. Polystyrene microplastics alter the behavior, energy reserve and nutritional composition of marine jacopever (*Sebastes schlegelii*) [J]. J Hazard Mater,2018 ,360:97–105.
31. Zheng W, Su H, Lv X, Xin S, Xu T. Exon-Intron Circular RNA circRNF217 Promotes Innate Immunity and Antibacterial Activity in Teleost Fish by Reducing miR-130-3p Function[J]. J Immunol ,2022,208(5):1099–1114.
32. Zhou X, Michal JJ, Zhang L, Ding B, Lunney JK, Liu B, Jiang Z. Interferon induced IFIT family genes in host antiviral defense[J]. Int J Biol Sci. 2013;9(2):200–208.

Figures

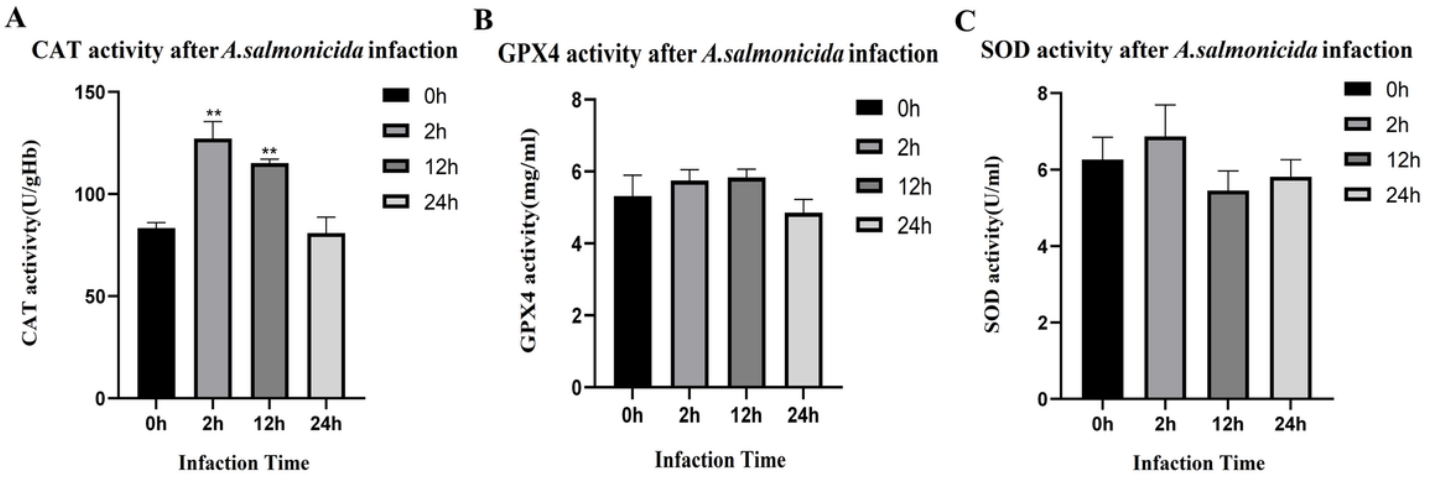

Figure 1

The CAT, GPX4 and SOD activities in the liver of *S. schlegelii* following *A. salmonicida* infection.

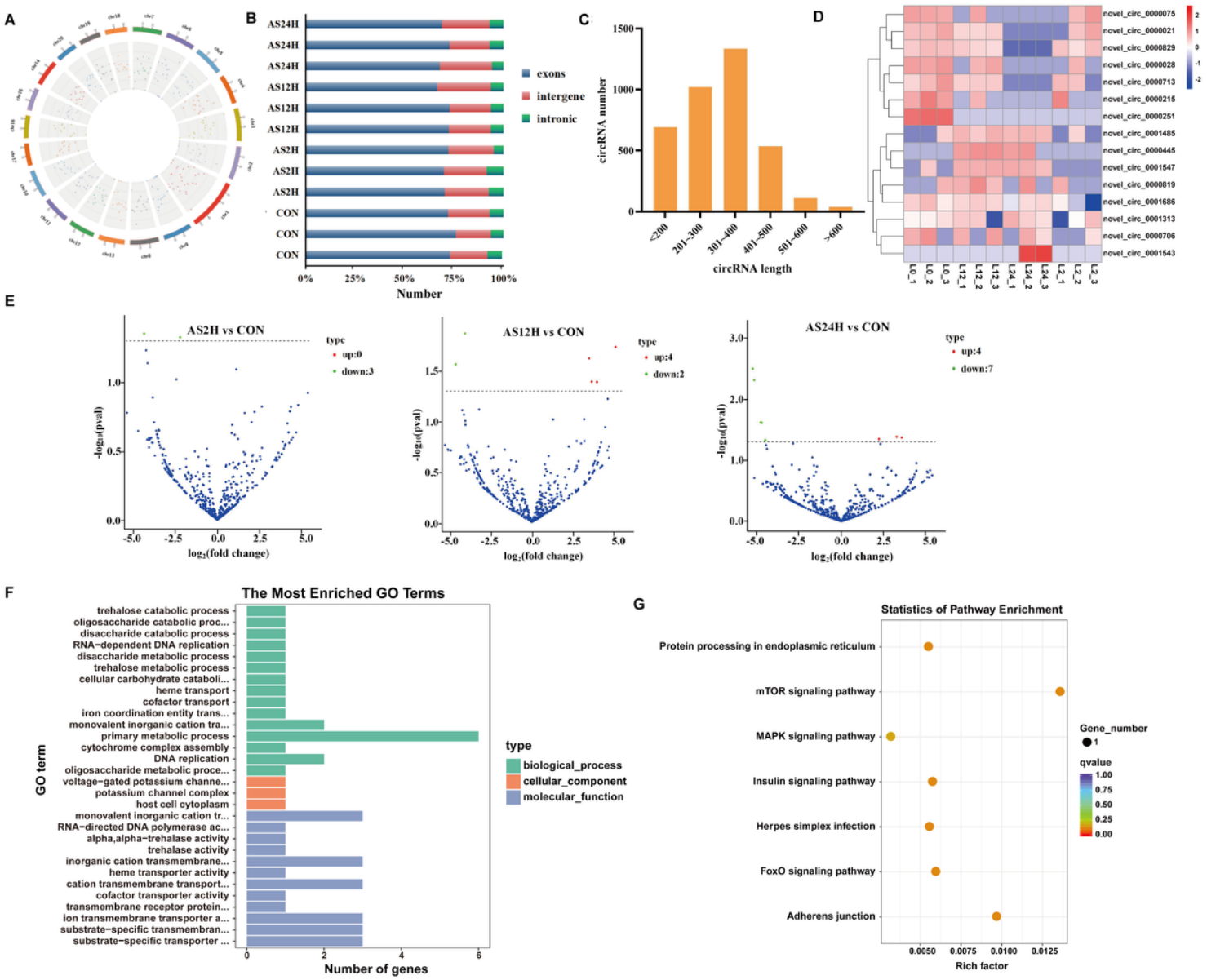

Figure 2

Features and characteristics of circRNAs in the liver of *S. schlegelii*, following *A. salmonicida* infection. (A-B) Chromosome locations of circRNAs; (C) The length distributions of identified circRNAs;(D) Expression patterns of circRNAs among control and infected groups; (E) Volcano plots of DE circRNAs among control and infected groups; (F) Go term analysis of DE circRNAs; (G) KEGG analysis of DE circRNAs.

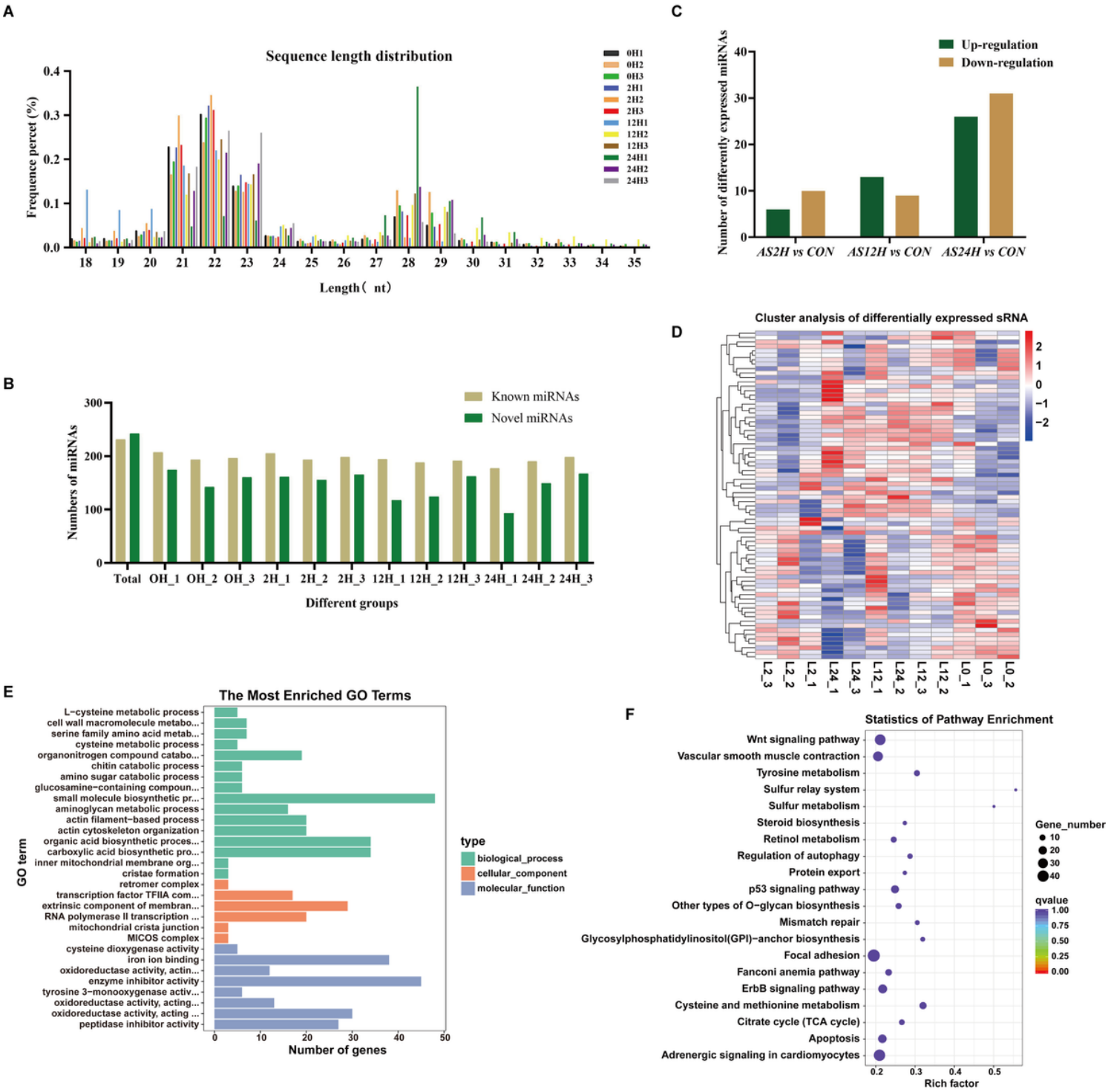

Figure 3

Features and characteristics of miRNAs in the liver of *S. schlegelii*, following *A. salmonicida* infection. (A-B) The length distribution of identified miRNAs; (C) The differently expressed miRNAs; (D) Expression patterns of miRNAs among control and infected groups; (E) Go term analysis of DE-miRNAs; (F) KEGG analysis of DE-miRNAs.

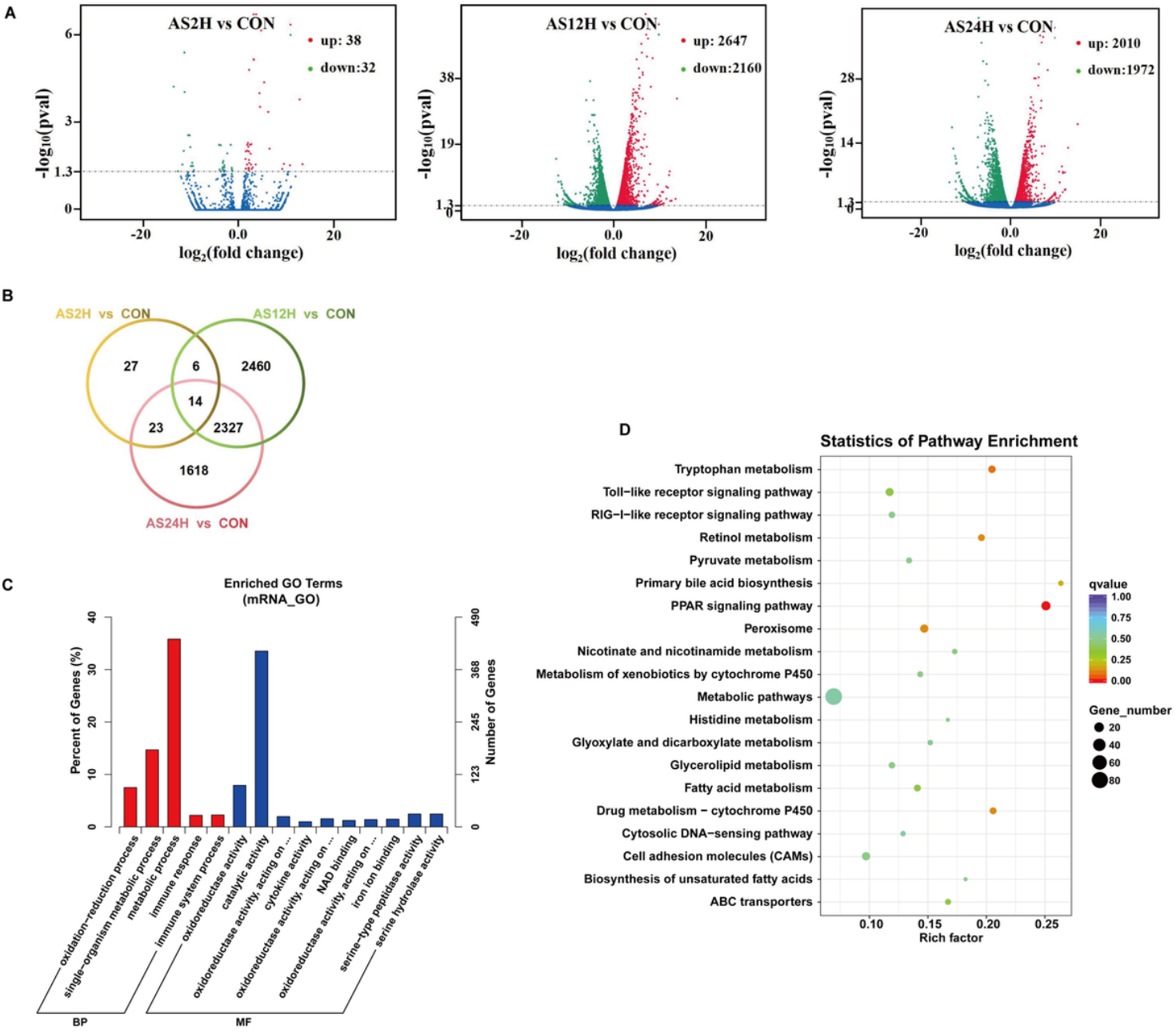

Figure 4

Features and characteristics of mRNAs in the liver of *S. schlegelii*, following *A. salmonicida* infection. (A) Volcano plots were drawn to visualize the standardized expression of mRNAs between the infected and control groups. The red and green points represent differentially expressed mRNAs with statistical significance (P < 0.05); (B) Veen diagram of mRNAs; (C) Go term analysis of DE-mRNAs; (D) KEGG analysis of DE-mRNAs.

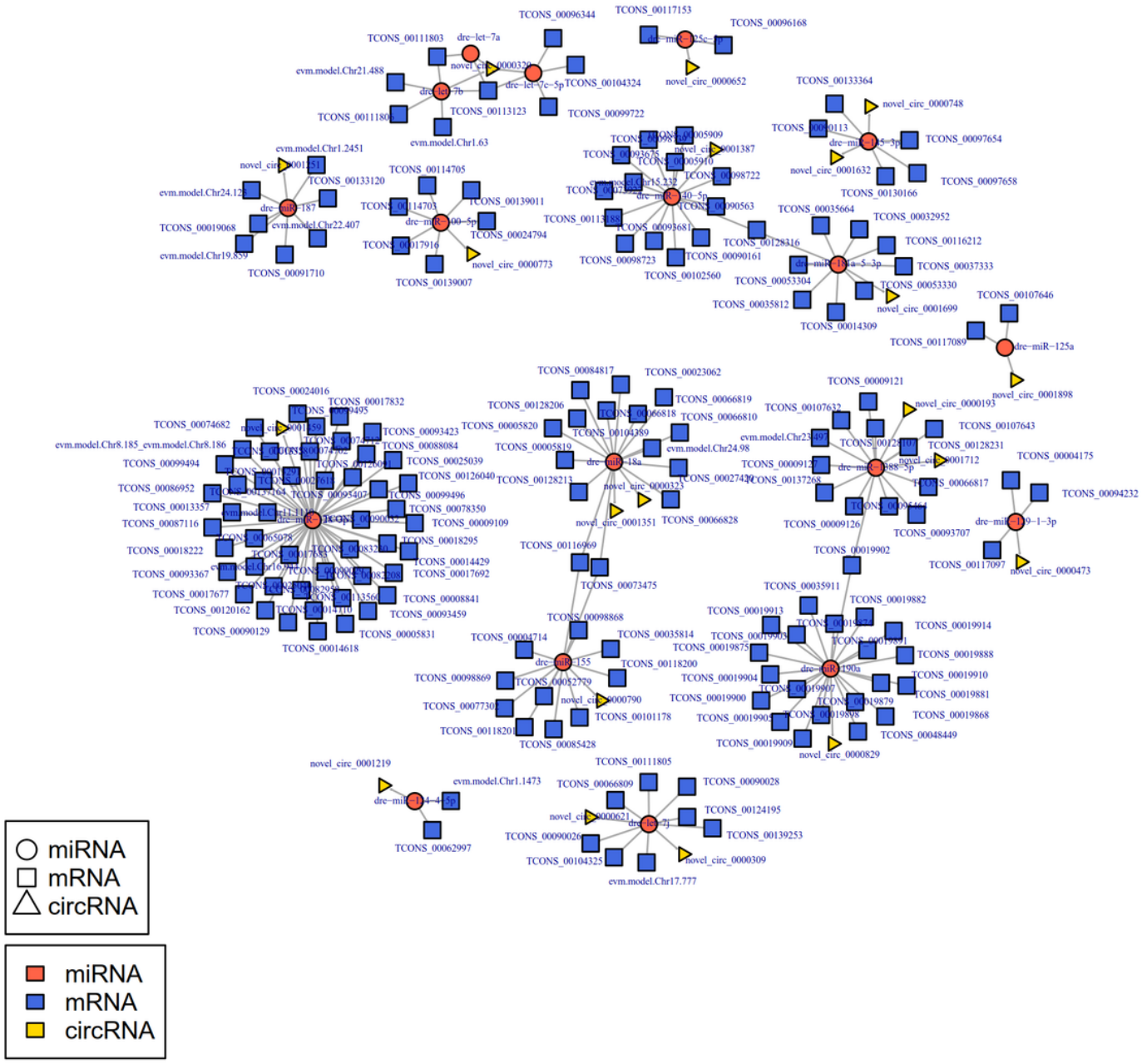

Figure 5

The ceRNA regulatory networks in the liver of *S. schlegelii* following *A. salmonicida* infection. Red circle nodes represent miRNAs, yellow triangle nodes represent circRNAs, and blue squares represent mRNAs.

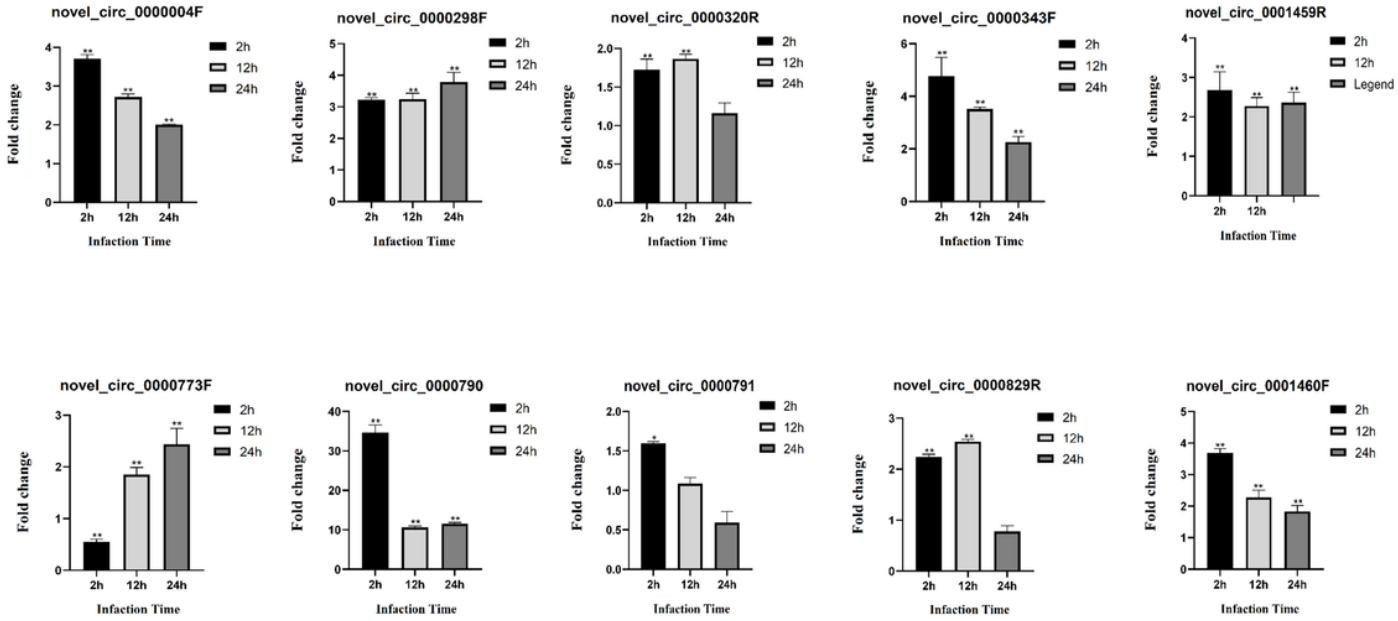

Figure 6

Validation of circRNAs by qRT-PCR. Error bars represent SE of expression levels of each circRNA. The relative expression level of circRNAs in 2 h, 12 h and 24 h were calculated as the ratio of the gene expression level (qRT-PCR). * on the bars represent $p < 0.05$ and ** represent $p < 0.01$ between *A. salmonicida* infected *S. schlegelii* and control groups (n = 3 for each group).

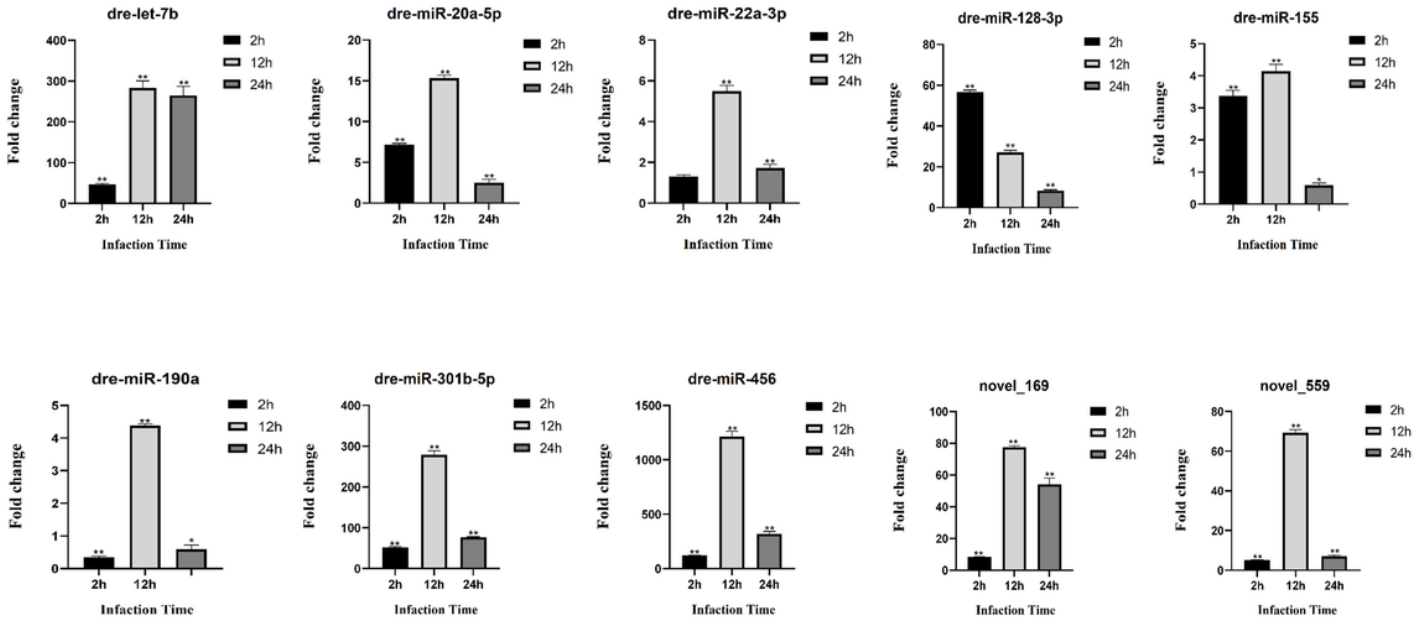

Figure 7

Validation of miRNAs by qRT-PCR. Error bars represent SE of expression levels of each miRNA. The relative expression level of miRNAs in 2 h, 12 h and 24 h were calculated as the ratio of the gene expression level (qRT-PCR). * on the bars represent $p < 0.05$ and ** represent $p < 0.01$ between *A. salmonicida* infected *S. schlegelii* and control groups (n = 3 for each group).

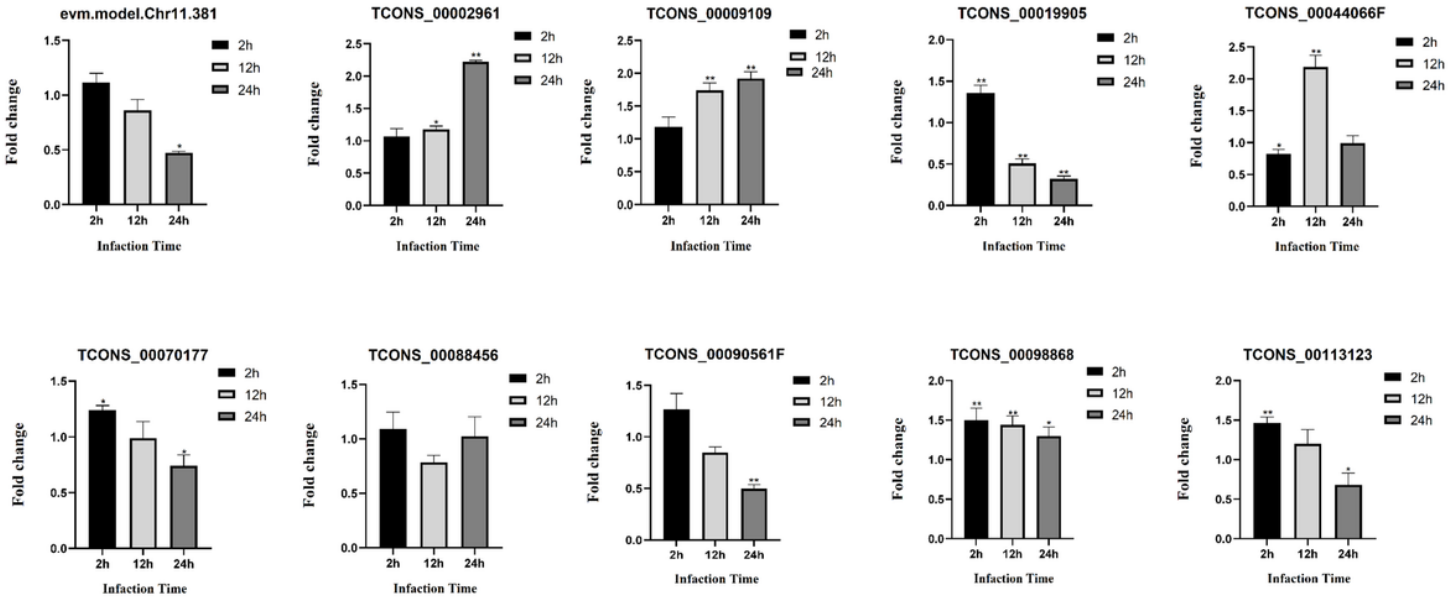

Figure 8

Validation of mRNAs by qRT-PCR. Error bars represent SE of expression levels of each mRNA. The relative expression level of mRNAs in 2 h, 12 h and 24 h were calculated as the ratio of the gene expression level (qRT-PCR). * on the bars represent $p < 0.05$ and ** represent $p < 0.01$ between *A. salmonicida* infected *S. schlegelii* and control groups (n = 3 for each group).

Supplementary Files

This is a list of supplementary files associated with this preprint. Click to download.

- Supplementaryfiles.zip